Multiscalar B-L extension based on S_4 flavor symmetry for neutrino masses and mixing*

V. V. Vien[1,2†] H. N. Long[3,4‡]

[1]Institute of Research and Development, Duy Tan University, 182 Nguyen Van Linh, Da Nang City, Vietnam
[2]Department of Physics, Tay Nguyen University, 567 Le Duan, Buon Ma Thuot, DakLak, Vietnam
[3]Theoretical Particle Physics and Cosmology Research Group, Advanced Institute of Materials Science, Ton Duc Thang University, Ho Chi Minh City, Vietnam
[4]Faculty of Applied Sciences, Ton Duc Thang University, Ho Chi Minh City, Vietnam

Abstract: A multiscalar and nonrenormalizable $B-L$ extension of the standard model (SM) with S_4 symmetry which successfully explains the recently observed neutrino oscillation data is proposed. The tiny neutrino masses and their hierarchies are generated via the type-I seesaw mechanism. The model reproduces the recent experiments of neutrino mixing angles and Dirac CP violating phase in which the atmospheric angle (θ_{23}) and the reactor angle (θ_{13}) get the best-fit values while the solar angle (θ_{12}) and Dirac CP violating phase (δ) are in 3σ range of the best-fit value for the normal hierarchy (NH). For the inverted hierarchy (IH), θ_{13} gets the best-fit value and θ_{23} together with δ are in the 1σ range, while θ_{12} is in 3σ range of the best-fit value. The effective neutrino masses are predicted to be $\langle m_{ee}\rangle = 6.81$ meV for the NH and $\langle m_{ee}\rangle = 48.48$ meV for the IH, in good agreement with the most recent experimental data.

Keywords: neutrino mass and mixing, extensions of electroweak Higgs sector, flavor symmetries

DOI: 10.1088/1674-1137/abe1c7

I. INTRODUCTION

The observed neutrino oscillation data, including the neutrino mass-squared differences, mixing angles, and the Dirac CP phases given in Table 1, is a subject of intense interest in current particle physics. This pattern provides inspiration for constructing models with additional scalars and symmetries and makes it interesting to extend the SM. Among the various extensions of the SM, the $B-L$ gauge model is one of the simplest extensions which has been studied in previous works [2-12], whereby the anomalies are canceled in different ways [13-15][1)]. In this work, we improve the model proposed in Refs. [7, 8], where neutrino masses and various other phenomena involving leptogenesis, dark matter, etc, are satisfied. It is emphasized that the above-mentioned model by itself cannot predict the recently observed neutrino oscillation data.

It is worth mentioning that non-Abelian discrete symmetries have revealed many outstanding issues. Consequently, many of them have been applied in explaining the observed neutrino oscillation pattern. One of them, the S_4 symmetry, has been widely used because it provides a viable description of the observed neutrino oscillation data [15-41]. However, the above-mentioned models contain non-minimal scalar sectors with many Higgs doublets. Thus, it is interesting to find an alternative extension which can give a better explanation of the observed neutrino oscillation data with less scalar content than previous models. In this work, we propose an alternative and improved version of the $B-L$ model with an additional flavor symmetry group, $S_4\otimes Z_3$, which accommodates the current neutrino oscillation data given in Table 1. In this work, all left-handed leptons are put in $\underline{3}$ while for the right-handed leptons, the first generation is

Received 8 December 2020; Accepted 29 January 2021; Published online 26 February 2021

* This research is funded by Vietnam National Foundation for Science and Technology Development (NAFOSTED) (103.01-2017.341)

† E-mail: wvienk16@gmail.com
‡ E-mail: hoangngoclong@tdtu.edu.vn, Corresponding author

1) The anomalies mentioned here are for continuous symmetries. Anomalies of non-Abelian discrete symmetries has been presented in the literature. The S_4 group is isomorphic to $(Z_2\otimes Z_2)\rtimes S_3$, and then the Z_2 symmetry of S_3 can be anomalous in S_4. Three representations $\underline{2}$, $\underline{3}$ and $\underline{1}'$ of S_4 have $\det\rho(g) = -1$ thus the odd number of $\underline{2}$, $\underline{3}$ and $\underline{1}'$ can lead to anomalies. However, in the model consideration, there is no irreducible representation $\underline{1}'$ is used and the number of irreducible representation $\underline{2}$, as well as the number of irreducible representation $\underline{3}$, of S_4 is even, therefore S_4 is an anomaly-free symmetry.

Table 1. Observed neutrino oscillation data taken from Ref. [1]. Here, $\Delta m^2_{3l} \equiv \Delta m^2_{31} > 0$ for NH and $\Delta m^2_{3l} \equiv \Delta m^2_{32} < 0$ for IH.

Parameters	NH		IH	
	bfp $\pm 1\sigma$	3σ range	bfp $\pm 1\sigma$	3σ range
$\sin^2\theta_{23}$	$0.573^{+0.016}_{-0.020}$	$0.415 \to 0.616$	$0.575^{+0.016}_{-0.019}$	$0.419 \to 0.617$
$\theta_{23}/(^\circ)$	$49.2^{+0.9}_{-1.2}$	$40.1 \to 51.7$	$49.3^{+0.9}_{-1.1}$	$40.3 \to 51.8$
$\sin^2\theta_{12}$	$0.304^{+0.012}_{-0.012}$	$0.269 \to 0.343$	$0.304^{+0.013}_{-0.012}$	$0.269 \to 0.343$
$\theta_{12}/(^\circ)$	$33.44^{+0.77}_{-0.74}$	$31.27 \to 35.86$	$33.45^{+0.78}_{-0.75}$	$31.27 \to 35.87$
$\sin^2\theta_{13}$	$0.02219^{+0.00062}_{-0.00063}$	$0.02032 \to 0.02410$	$0.02238^{+0.00063}_{-0.00062}$	$0.02052 \to 0.02428$
$\theta_{13}/(^\circ)$	$8.57^{+0.12}_{-0.12}$	$8.20 \to 8.93$	$8.60^{+0.12}_{-0.12}$	$8.24 \to 8.96$
$\delta_{CP}(^\circ)$	197^{+27}_{-24}	$120 \to 369$	282^{+26}_{-30}	$193 \to 352$
$\frac{\Delta m^2_{21}}{10^{-5}\,\mathrm{eV}^2}$	$7.42^{+0.21}_{-0.20}$	$6.82 \to 8.04$	$7.42^{+0.21}_{-0.20}$	$6.82 \to 8.04$
$\frac{\Delta m^2_{3l}}{10^{-3}\,\mathrm{eV}^2}$	$+2.517^{+0.026}_{-0.028}$	$+2.435 \to +2.598$	$-2.498^{+0.028}_{-0.028}$	$-2.581 \to -2.414$

put in $\underline{1}$ and the two others are in $\underline{2}$. The S_4 group contains 24 elements dispensed into five conjugacy classes and five irreducible representations, denoted as $\underline{1}$, $\underline{1}'$, $\underline{2}$, $\underline{3}$, and $\underline{3}'$. In this paper, we work in the basis where $\underline{3}$ and $\underline{3}'$ are real whereas $\underline{2}$ is complex. For a detailed description of the S_4 group, the reader is referred to Ref. [15]. Despite the S_4 symmetry being previously studied in various works [15-41], to the best of our knowledge, this symmetry has not been considered before in the $B-L$ scenario.

This paper is arranged as follows. The model is described in Section II. Section III is devoted to neutrino mass and mixing. The results of the numerical analysis are presented in Section IV and finally, some conclusions are given in Section V.

II. THE MODEL

The full symmetry of the model is $G = G_{\rm SM} \otimes U(1)_{B-L} \otimes S_4 \otimes Z_3$, where $G_{\rm SM} = SU(3)_{\rm C} \otimes SU(2)_{\rm L} \otimes U(1)_{\rm Y}$ is the gauge group of the SM. In this model, the first generation of right-handed leptons is put in $\underline{1}$ while the two others are put in $\underline{2}$ under S_4 and the three generations of left-handed leptons as well as the three right-handed neutrinos are put in $\underline{3}$. The model particle content is given in Table 2, where ϕ, ϕ' and η are S_4 triplets whose components are $SU(2)_{\rm L}$ singlets, and χ is one S_4 doublet whose components are $SU(2)_{\rm L}$ singlets.

Under G symmetry, $\bar{\psi}_{\rm L} l_{1\rm R}$ and $\bar{\psi}_{\rm L} l_{\alpha\rm R}$ transform as $(1,2,-1/2,0,\underline{3},\omega^2)$ and $(1,2,-1/2,0,\underline{3}\oplus\underline{3}',\omega^2)$, respectively. Thus, we need one $SU(2)_{\rm L}$ doublet H and two $SU(2)_{\rm L}$ singlets ϕ, ϕ', as presented in Table 2, to generate

Table 2. The model particle and scalar contents ($\alpha = 2,3$).

Fields	$\psi_{\rm L}$	$l_{1\rm R}(l_{\alpha\rm R})$	$\nu_{\rm R}$	H	ϕ	ϕ'	χ	η
$SU(3)_{\rm C}$	**1**	**1**	**1**	**1**	**1**	**1**	**1**	**1**
$SU(2)_{\rm L}$	**2**	**1**	**1**	**2**	**1**	**1**	**1**	**1**
$U(1)_{\rm Y}$	$-\frac{1}{2}$	-1	0	$\frac{1}{2}$	0	0	0	0
$U(1)_{B-L}$	-1	-1	-1	0	0	0	2	2
S_4	$\underline{3}$	$\underline{1}(\underline{2})$	$\underline{3}$	$\underline{1}$	$\underline{3}$	$\underline{3}'$	$\underline{2}$	$\underline{3}$
Z_3	ω^2	ω	ω^2	1	ω	ω	ω^2	ω^2

masses for the charged leptons.

Furthermore, the neutrino masses arise from $\bar{\psi}_{\rm L}\nu_{\rm R}$ and $\bar{\nu}^c_{\rm R}\nu_{\rm R}$ to scalars, where under G symmetry, $\bar{\psi}_{\rm L}\nu_{\rm R} \sim (1,2,1/2,0,\underline{1}\oplus\underline{2}\oplus\underline{3}\oplus\underline{3}',1)$ and $\bar{\nu}^c_{\rm R}\nu_{\rm R} \sim (1,1,0,-2,\underline{1}\oplus\underline{2}\oplus\underline{3}\oplus\underline{3}',\omega)$. For the known scalars (H,ϕ,ϕ'), under G symmetry, there is only one invariant term $(\bar{\psi}_{\rm L}\nu_{\rm R})_{\underline{1}}\widetilde{H}$ which is responsible for generating Dirac masses for the neutrinos. In order to generate realistic neutrino masses and mixings, we add two singlets χ, η, respectively put in $\underline{2}$ and $\underline{3}$ under S_4 coupling to $\bar{\nu}^c_{\rm L}\nu_{\rm R}$ which are responsible for generating Majorana masses for the neutrinos.

Up to five dimensions, the Yukawa couplings invariant under all symmetries are[1)]

$$\begin{aligned} -\mathcal{L}_l = {} & \frac{h_1}{\Lambda}(\bar{\psi}_{\rm L} l_{1\rm R})_{\underline{3}}(H\phi)_{\underline{3}} + \frac{h_2}{\Lambda}(\bar{\psi}_{\rm L} l_{\alpha\rm R})_{\underline{3}}(H\phi)_{\underline{3}} \\ & + \frac{h_3}{\Lambda}(\bar{\psi}_{\rm L} l_{\alpha\rm R})_{\underline{3}'}(H\phi')_{\underline{3}'} + x(\bar{\psi}_{\rm L}\nu_{\rm R})_{\underline{1}}\widetilde{H} \\ & + \frac{y}{2}(\bar{\nu}^c_{\rm R}\nu_{\rm R})_{\underline{2}}\chi + \frac{z}{2}(\bar{\nu}^c_{\rm R}\nu_{\rm R})_{\underline{3}}\eta + \text{H.c}, \end{aligned} \tag{1}$$

1) In fact, there exist the other contributions via higher dimensional Weinberg operators, such as $\frac{1}{\Lambda^{2(n+m+1)}}\overline{\psi}^c_{\rm L}\psi_{\rm L}H^2X(H^\dagger H)^m(X^\dagger X)^n$ with $m,n = 0,1,2,...$; $X = \chi,\eta$ and Λ is the cutoff scale. However, since v_H and v_X are far smaller than the cutoff scale Λ, i.e., $v_H \ll v_X \ll \Lambda$. Thus, the left-handed neutrino mass generated via Type II seesaw mechanism $\sim v_H\left(\frac{v_H}{\Lambda}\right)^{2m+1}\left(\frac{v_X}{\Lambda}\right)^{2n+1}$ is very small compared to the one generated via the canonical type-I seesaw mechanism as in Eq. (13) and therefore would be neglected.

where Λ is the cut-off scale of the theory, and $h_{1,2,3}$ as well as x, y, z are the dimensionless Yukawa coupling constants.

To generate a suitable neutrino oscillation pattern, the following structure of VEVs is chosen:

$$\begin{aligned}\langle H\rangle^T =&(0v_H), \langle\phi\rangle = (\langle\phi_1\rangle, \langle\phi_1\rangle, \langle\phi_1\rangle), \langle\phi_1\rangle = v_\phi,\\ \langle\phi^{'}\rangle =&(\langle\phi^{'}_1\rangle, \langle\phi^{'}_1\rangle, \langle\phi^{'}_1\rangle), \langle\phi^{'}_1\rangle = v_{\phi^{'}},\\ \langle\eta\rangle =&(0, 0, \langle\eta_3\rangle), \langle\eta_3\rangle = v_\eta,\\ \langle\chi\rangle =&(\langle\chi_1\rangle, \langle\chi_2\rangle), \langle\chi_{1,2}\rangle = v_{\chi_{1,2}}.\end{aligned} \tag{2}$$

The VEVs of ϕ and $\phi^{'}$, respectively, break S_4 down to S_3 and Z_3, while the VEVs of χ and η break S_4 down to the Klein four group K_4.

From Eq. (1), with expansion $\phi_i = \langle\phi_i\rangle + \phi^{'}_i$ and $H = (H^+ H^0)^T$, we get the lepton flavor changing interactions:

$$\begin{aligned}-\mathcal{L}_{\rm clep} \supset& \frac{h_1 v_\phi}{\Lambda}(\bar{l}_{2\rm L}H^0 + \bar{\nu}_{2\rm L}H^+)l_{1\rm R} + \frac{h_1 v_\phi}{\Lambda}(\bar{l}_{3\rm L}H^0\\ &+ \bar{\nu}_{3\rm L}H^+)l_{1\rm R} + \frac{h_2 v_\phi}{\Lambda}(\bar{l}_{1\rm L}H^0 + \bar{\nu}_{1\rm L}H^+)l_{2\rm R}\\ &+ \frac{h_2 v_\phi}{\Lambda}(\bar{l}_{1\rm L}H^0 + \bar{\nu}_{1\rm L}H^+)l_{3\rm R} - \frac{h_3 v_{\phi^{'}}}{\Lambda}(\bar{l}_{1\rm L}H^0\\ &+ \bar{\nu}_{1\rm L}H^+)l_{2\rm R} + \frac{h_3 v_{\phi^{'}}}{\Lambda}(\bar{l}_{1\rm L}H^0 + \bar{\nu}_{1\rm L}H^+)l_{3\rm R} + \text{H.c}.\end{aligned} \tag{3}$$

Equation (3) shows that, in the case $v_{\phi^{'}} \simeq v_\phi$, the usual Yukawa couplings are proportional to $\frac{v_\phi}{\Lambda}$ and the lepton flavor changing processes in this model are suppressed by the factor[1] $\frac{v_\phi}{\Lambda G_F^2 M_H^2}$ associated with the above small Yukawa couplings and the large mass scale of the heavy scalars. For further details, the reader is referred to Refs. [42-45]. Furthermore, this model contains only one $SU(2)_{\rm L}$ Higgs doublet; therefore, the flavor changing neutral current processes are absent at tree level.

III. NEUTRINO MASS AND MIXING

From the Yukawa interactions in Eq. (1), using the tensor product of S_4 [15], together with the VEVs of H, ϕ and $\phi^{'}$ in Eq. (2), the charged lepton mass terms are written as follows:

$$\mathcal{L}_{cl}^{\rm mass} = -(\bar{l}_{1\rm L}\bar{l}_{2\rm L}\bar{l}_{3\rm L})M_l(l_{1\rm R}l_{2\rm R}l_{3\rm R})^T + \text{H.c}, \tag{4}$$

where

$$M_l = \frac{v_H}{\Lambda}\begin{pmatrix} h_1 v_\phi & h_2 v_\phi - h_3 v_{\phi^{'}} & h_2 v_\phi + h_3 v_{\phi^{'}}\\ h_1 v_\phi & \omega^2(h_2 v_\phi - h_3 v_{\phi^{'}}) & \omega(h_2 v_\phi + h_3 v_{\phi^{'}})\\ h_1 v_\phi & \omega(h_2 v_\phi - h_3 v_{\phi^{'}}) & \omega^2(h_2 v_\phi + h_3 v_{\phi^{'}})\end{pmatrix}. \tag{5}$$

The matrix M_l is diagonalized as $U_l^\dagger M_l U_r = \text{diag}(m_e, m_\mu, m_\tau)$, where

$$U_{\rm L}^\dagger = \frac{1}{\sqrt{3}}\begin{pmatrix}1 & 1 & 1\\ 1 & \omega & \omega^2\\ 1 & \omega^2 & \omega\end{pmatrix}, \quad U_{\rm R} = I_{3\times 3}, \quad \omega = e^{i2\pi/3}, \tag{6}$$

$$m_e = \frac{\sqrt{3}h_1 v_H v_\phi}{\Lambda}, \quad m_{\mu,\tau} = \frac{\sqrt{3}v_H}{\Lambda}\left(h_2 v_\phi \mp h_3 v_{\phi^{'}}\right). \tag{7}$$

The left-handed mixing matrix $U_{\rm L}$ is non-trivial in our model and hence will contribute to the leptonic mixing matrix. Equation (7) shows that m_μ and m_τ are differentiated by $\phi^{'}$. This is why $\phi^{'}$ is additionally introduced to ϕ in the charged-lepton sector. Now, comparing the result in Eq. (7) with the best fit values for the masses of charged leptons taken from Ref. [46], $m_e \simeq 0.511$ MeV, $m_\mu \simeq 105.66$ MeV, and $m_\tau \simeq 1776.86$ MeV, we find the relations $\frac{h_1 v_H v_\phi}{\Lambda} = 0.295$ MeV, $\frac{h_2 v_H v_\phi}{\Lambda} = 543$ MeV, $\frac{h_3 v_H v_{\phi^{'}}}{\Lambda} = 482$ MeV, i.e., $h_1 : h_2 : h_3 \sim 1.00 : 1.840\times 10^3 : 1.634\times 10^3$.

Regarding the neutrino sector, from the Yukawa terms in Eq. (1) and using the tensor product of S_4 [15], the Yukawa Lagrangian invariant under G symmetry in the neutrino sector reads:

$$\begin{aligned}-\mathcal{L}_\nu =& x(\bar{\psi}_{1\rm L}\nu_{1\rm R} + \bar{\psi}_{2\rm L}\nu_{2\rm R} + \bar{\psi}_{2\rm L}\nu_{3\rm R})\widetilde{H}\\ &+ \frac{y}{2}\left[(\chi_1 + \chi_2)\bar{\nu}^c_{1\rm R}\nu_{1\rm R} + \omega(\omega\chi_1 + \chi_2)\bar{\nu}^c_{2\rm R}\nu_{2\rm R}\right.\\ &\left.+\omega(\chi_1 + \omega\chi_2)\bar{\nu}^c_{3\rm R}\nu_{3\rm R}\right]\\ &+ \frac{z}{2}\left[(\bar{\nu}^c_{2\rm R}\nu_{3\rm R} + \bar{\nu}^c_{3\rm R}\nu_{2\rm R})\eta_1 + (\bar{\nu}^c_{3\rm R}\nu_{1\rm R} + \bar{\nu}^c_{1\rm R}\nu_{3\rm R})\eta_2\right.\\ &\left.+ (\bar{\nu}^c_{1\rm R}\nu_{2\rm R} + \bar{\nu}^c_{2\rm R}\nu_{1\rm R})\eta_3\right] + \text{H.c}.\end{aligned} \tag{8}$$

After symmetry breaking, the mass Lagrangian for the neutrinos takes the following form:

$$-\mathcal{L}_\nu^{\rm mass} = \frac{1}{2}\bar{\chi}^c_{\rm L}M_\nu\chi_{\rm L} + \text{H.c}, \tag{9}$$

where

$$\begin{aligned}&\chi_{\rm L} = \left(\nu_{\rm L}\ \ \nu^c_{\rm R}\right)^T, \quad M_\nu = \begin{pmatrix}0 & M_D^T\\ M_D & M_{\rm R}\end{pmatrix},\\ &\nu_{\rm L} = (\nu_{1\rm L}\ \ \nu_{2\rm L}\ \ \nu_{3\rm L})^T, \quad \nu^c_{\rm R} = (\nu^c_{1\rm R}\ \ \nu^c_{2\rm R}\ \ \nu^c_{3\rm R})^T,\end{aligned} \tag{10}$$

1) Here, $G_F = g^2/(4\sqrt{2}m_W^2)$ and M_H is the mass scale of the heavy scalars providing the dominant contributions to the lepton flavor violation decays.

and the mass matrices M_D, $M_{\rm R}$ take the following forms:

$$\begin{aligned} M_D =& {\rm diag}(a_D, a_D, a_D),\\ M_{\rm R} =& \begin{pmatrix} a_{1\rm R}+a_{2\rm R} & a_{\rm R} & 0 \\ a_{\rm R} & \omega(\omega a_{1\rm R}+a_{2\rm R}) & 0 \\ 0 & 0 & \omega(a_{1\rm R}+\omega a_{2\rm R}) \end{pmatrix}, \end{aligned} \tag{11}$$

where

$$a_D = x v_\phi^*, \quad a_{1,2\rm R} = y v_{\chi_{1,2}}, \quad a_{\rm R} = z v_\eta. \tag{12}$$

In the seesaw mechanism, the effective neutrino mass matrix is given by

$$M_{\rm eff} = -M_D^T M_R^{-1} M_D = \begin{pmatrix} A_1+iA_2 & A_7+iA_8 & 0 \\ A_7+iA_8 & A_3+iA_4 & 0 \\ 0 & 0 & A_5+iA_6 \end{pmatrix}, \tag{13}$$

where

$$\begin{aligned} A_1A_0 =& -\left[2(a_{1\rm R}^3+a_{2\rm R}^3)+(a_{1\rm R}+a_{2\rm R})a_{\rm R}^2\right]a_D^2,\\ A_2A_0 =& \sqrt{3}(a_{2\rm R}-a_{1\rm R})a_D^2a_{\rm R}^2,\\ A_3A_0 =& (a_{1\rm R}+a_{2\rm R})a_D^2[(a_{1\rm R}+a_{2\rm R})^2+2a_{\rm R}^2],\\ A_4A_0 =& \sqrt{3}(a_{2\rm R}-a_{1\rm R})(a_{1\rm R}+a_{2\rm R})^2a_D^2,\\ A_5 =& \frac{(a_{1\rm R}+a_{2\rm R})a_D^2}{2\left(a_{1\rm R}^2-a_{1\rm R}a_{2\rm R}+a_{2\rm R}^2\right)},\\ A_6 =& \frac{\sqrt{3}}{2}\frac{(a_{2\rm R}-a_{1\rm R})a_D^2}{a_{1\rm R}^2-a_{1\rm R}a_{2\rm R}+a_{2\rm R}^2},\\ A_7A_0 =& -a_D^2a_{\rm R}\left[(a_{1\rm R}+a_{2\rm R})^2+2a_{\rm R}^2\right],\\ A_8A_0 =& \sqrt{3}(a_{1\rm R}^2-a_{2\rm R}^2)a_D^2a_{\rm R},\\ A_0 =& 2\Big[a_{1\rm R}^4+a_{1\rm R}^3a_{2\rm R}\\ &+a_{1\rm R}a_{2\rm R}^3+a_{2\rm R}^4+(a_{1\rm R}+a_{2\rm R})^2a_{\rm R}^2+a_{\rm R}^4\Big]. \end{aligned} \tag{14}$$

Let us first define a Hermitian matrix $\mathcal{M}^2$, given by

$$M^2 = M_{\rm eff}M_{\rm eff}^+ = \begin{pmatrix} a_0 & d_0+{\rm i}g_0 & 0 \\ d_0-{\rm i}g_0 & b_0 & 0 \\ 0 & 0 & c_0 \end{pmatrix}, \tag{15}$$

where

$$\begin{aligned} a_0 =& a_1^2+a_2^2+a_7^2+a_8^2+2a_1a_2\sin(\alpha_1-\alpha_2)\\ &+2a_7a_8\sin(\alpha_7-\alpha_8),\\ b_0 =& a_3^2+a_4^2+a_7^2+a_8^2+2a_3a_4\sin(\alpha_3-\alpha_4)\\ &+2a_7a_8\sin(\alpha_7-\alpha_8),\\ c_0 =& a_5^2+a_6^2+2a_5a_6\sin(\alpha_5-\alpha_6),\\ d_0 =& a_7[a_1\cos(\alpha_1-\alpha_7)-a_2\sin(\alpha_2-\alpha_7)\\ &+a_3\cos(\alpha_3-\alpha_7)+a_4\sin(\alpha_4-\alpha_7)]\\ &+a_8[a_1\sin(\alpha_1-\alpha_8)+a_2\cos(\alpha_2-\alpha_8)\\ &+a_3\sin(\alpha_3-\alpha_8)+a_4\cos(\alpha_4-\alpha_8)],\\ g_0 =& a_7[a_1\sin(\alpha_1-\alpha_7)+a_2\cos(\alpha_2-\alpha_7)\\ &-a_3\cos(\alpha_3-\alpha_7)-a_4\sin(\alpha_4-\alpha_7)]\\ &-a_8[a_1\cos(\alpha_1-\alpha_8)-a_2\sin(\alpha_2-\alpha_8)\\ &-a_3\cos(\alpha_3-\alpha_8)+a_4\sin(\alpha_4-\alpha_8)], \end{aligned} \tag{16}$$

with $a_i = |A_i|$ and $\alpha_i\,(i = 1-8)$ being the arguments of A_i.

The squared-mass matrix $\mathcal{M}^2$ in Eq. (15) has three exact eigenvalues:

$$m_1 = \kappa_1-\kappa_2, \;\; m_2 = c_0, \;\; m_3 = \kappa_1+\kappa_2, \tag{17}$$

with

$$2\kappa_1 = a_0+b_0, \;\; 2\kappa_2 = \sqrt{(a_0-b_0)^2+4(d_0^2+g_0^2)}, \tag{18}$$

and the corresponding mixing matrix is

$$U = \begin{pmatrix} \cos\theta & 0 & -\sin\theta{\rm e}^{{\rm i}\alpha} \\ 0 & 1 & 0 \\ \sin\theta{\rm e}^{-{\rm i}\alpha} & 0 & \cos\theta \end{pmatrix}, \tag{19}$$

with

$$\begin{aligned} \alpha =& -{\rm i}\ln\left(-\frac{d_0+{\rm i}g_0}{\sqrt{d_0^2+g_0^2}}\right),\\ \theta =& \arcsin\left(\frac{1}{K^2+1}\right), \end{aligned} \tag{20}$$

$$K = \frac{b_0-m_1}{\sqrt{d_0^2+g_0^2}} = \frac{m_3-a_0}{\sqrt{d_0^2+g_0^2}}. \tag{21}$$

The sign of Δm_{31}^2 plays a pivotal role in the form of the neutrino mass hierarchy. In the NH, $m_1 \ll m_2 \sim m_3$, and thus the lightest neutrino mass is m_1, while in the IH, $m_3 \ll m_1 \sim m_2$, thus the lightest neutrino mass is m_3 [46]. The neutrino mass matrix $M_{\rm eff}$ in Eq. (13) is diagonalized as

$$U_\nu^+ \mathcal{M}^2 U_\nu = \begin{cases} \begin{pmatrix} m_1 & 0 & 0 \\ 0 & m_2 & 0 \\ 0 & 0 & m_3 \end{pmatrix}, U_\nu = \begin{pmatrix} \cos\theta & 0 & -\sin\theta e^{i\alpha} \\ \sin\theta e^{-i\alpha} & 0 & \cos\theta \\ 0 & 1 & 0 \end{pmatrix} \text{ for NH}, \\ \begin{pmatrix} m_3 & 0 & 0 \\ 0 & m_2 & 0 \\ 0 & 0 & m_1 \end{pmatrix}, U_\nu = \begin{pmatrix} \sin\theta e^{i\alpha} & 0 & \cos\theta \\ -\cos\theta & 0 & \sin\theta e^{-i\alpha} \\ 0 & 1 & 0 \end{pmatrix} \text{ for IH}, \end{cases} \tag{22}$$

where $m_{2,3}$ and α, θ are given in Eqs. (17) and (20), respectively. The corresponding leptonic mixing matrix is

$$U_{\rm lep} = U_{\rm L}^\dagger U_\nu = \begin{cases} \frac{1}{\sqrt{3}} \begin{pmatrix} \cos\theta + \sin\theta.e^{-i\alpha} & 1 & \cos\theta - \sin\theta.e^{i\alpha} \\ \cos\theta + \omega\sin\theta.e^{-i\alpha} & \omega^2 & \omega\cos\theta - \sin\theta.e^{i\alpha} \\ \cos\theta + \omega^2\sin\theta.e^{-i\alpha} & \omega & \omega^2\cos\theta - \sin\theta.e^{i\alpha} \end{pmatrix} \text{ for NH}, \\ \frac{1}{\sqrt{3}} \begin{pmatrix} -\cos\theta + \sin\theta.e^{i\alpha} & 1 & \cos\theta + \sin\theta.e^{-i\alpha} \\ -\omega\cos\theta + \sin\theta.e^{i\alpha} & \omega^2 & \cos\theta + \omega\sin\theta.e^{-i\alpha} \\ -\omega^2\cos\theta + \sin\theta.e^{i\alpha} & \omega & \cos\theta + \omega^2\sin\theta.e^{-i\alpha} \end{pmatrix} \text{ for IH}. \end{cases} \tag{23}$$

In the three-neutrino scheme, lepton mixing angles can be defined as:

$$s_{13}^2 = |U_{e3}|^2, \quad t_{12}^2 = \left|\frac{U_{e2}}{U_{e1}}\right|^2, \quad t_{23}^2 = \left|\frac{U_{\mu 3}}{U_{\tau 3}}\right|^2, \tag{24}$$

where $t_{12} = s_{12}/c_{12}$, $t_{23} = s_{23}/c_{23}$, $c_{ij} = \cos\theta_{ij}$, $s_{ij} = \sin\theta_{ij}$ with θ_{ij} are neutrino mixing angles.

Combining the standard parametrization of the lepton mixing matrix [47-54] and Eq. (23), the Jarlskog invariant constraining the size of CP violation in lepton sector is determined as [52-54]:

$$J_{\rm CP} = {\rm Im}(U_{12}U_{23}U_{13}^*U_{22}^*) = \begin{cases} -\frac{\cos(2\theta)}{6\sqrt{3}} & \text{for NH}, \\ \frac{\cos(2\theta)}{6\sqrt{3}} & \text{for IH}. \end{cases} \tag{25}$$

Equations (23), (24) and (25) yield the following relations:

$$\cos\theta = \begin{cases} \sqrt{\frac{1}{2} - 3\sqrt{3}J_{\rm CP}} & \text{for NH}, \\ \sqrt{\frac{1}{2} + 3\sqrt{3}J_{\rm CP}} & \text{for IH}. \end{cases}, \tag{26}$$

$$\cos\alpha = \begin{cases} \frac{1 - 3s_{13}^2}{\sqrt{1 - 108J_{\rm CP}^2}} & \text{for NH}, \\ \frac{-1 + 3s_{13}^2}{\sqrt{1 - 108J_{\rm CP}^2}} & \text{for IH}. \end{cases}, \tag{27}$$

$$\sin\delta = -\frac{1}{2}\sqrt{4 - O(s_{13}^2, s_{23}^2)} \text{ for both NH and IH}, \tag{28}$$

$$O(s_{13}^2, s_{23}^2) = \frac{(1-2s_{13}^2)^2(1-2s_{23}^2)^2}{s_{13}^2 s_{23}^2(2-3s_{13}^2)(1-s_{23}^2)}, \tag{29}$$

$$t_{12}^2 = \frac{1}{2 - 3s_{13}^2} \text{ for both NH and IH}. \tag{30}$$

Since s_{13}^2 is a very small positive number and s_{23}^2 is very close to $\frac{1}{2}$, we can approximate that $O(s_{13}^2, s_{23}^2) \ll 1$. Thus, from Eqs. (28)-(30) we can approximate

$$t_{12}^2 > \frac{1}{2}, \quad \sin\delta \simeq -1 + \frac{O(s_{13}^2, s_{23}^2)}{8} < 0. \tag{31}$$

From Eqs. (17), (22) and (23), one can determine the effective neutrino masses governing beta decay (m_β) and neutrinoless double beta decay ($\langle m_{ee}\rangle$), which can in principle determine the absolute neutrino mass scale [55-57]:

$$m_\beta = \sqrt{\sum_{i=1}^{3} |U_{ei}|^2 m_i^2}, \quad \langle m_{ee}\rangle = \left|\sum_{i=1}^{3} U_{ei}^2 m_i\right|, \tag{32}$$

where $m_i\,(i = 1,2,3)$ are the masses of the three active neutrinos defined from Eqs. (17) and (22) while U_{ei} are the elements of $U_{\rm PMNS}$ determined from Eq. (23).

IV. NUMERICAL ANALYSIS

In the 1σ range[1)] [1], $s_{13} \in (0.1468, 0.1510)$ and $s_{23} \in (0.7436, 0.7675)$ for NH, while $s_{13} \in (0.1475, 0.1517)$ and

1) Here, numbers are displayed with 4 significant digits to the right of the decimal point.

$s_{23} \in (0.7457, 0.7688)$ for IH. Thus, from Eqs. (1) and (2) we can find the range of values of $\cos\theta$ and $\cos\alpha$ as plotted in Figs. 1, 2 and 3, respectively. On the other hand, since s^2_{13} is a very small and s^2_{23} is very close to $\frac{1}{2}$, we can assume $O(s^2_{13}, s^2_{23}) \ll 1$. Thus, from Eqs. (28) and (29) we can approximate

$$\sin\delta \simeq -1 + \frac{O(s^2_{13}, s^2_{23})}{8} < 0. \tag{33}$$

Figure 3 shows that, in the 1σ range of the best-fit value taken from Ref. [1], the range of the Dirac CP violating phase is defined as

$$\sin\delta \in \begin{cases} (-0.8664, -0.5688) \text{ for NH}, \\ (-0.8509, -0.5462) \text{ for IH}, \end{cases} \tag{34}$$

i.e.,

$$\delta \in \begin{cases} (299.96, 325.33)^\circ \text{ for NH}, \\ (301.70, 326.90)^\circ \text{ for IH}. \end{cases} \tag{35}$$

In the case where θ_{23} takes its maximal values ($\theta_{23} = \frac{\pi}{4}$), $O(s^2_{13}, s^2_{23}) = 0$ and $\sin\delta = -1$, the model predicts the cobimaximal mixing pattern [58-69]: $\theta_{13} \neq 0$, $\theta_{23} = \frac{\pi}{4}$ and $\delta = -\frac{\pi}{2}$. Furthermore, Eq. (30) implies $t_{12} \in (0.7188, 0.7195)$ for NH and $t_{12} \in (0.7189, 0.7196)$ for IH in the 1σ range of s_{13} of the best-fit value taken from Ref. [1], which is plotted in Fig. 4. These intervals of θ_{12} are in 3σ range of the best-fit value.

Figure 3 shows that, in our model, $\sin\delta \in (-0.851, -0.546)$, i.e. $\delta^\circ \in (300.0, 325)$, for NH, and $\sin\delta \in (-0.866, -0.569)$, i.e., $\delta^\circ \in (301.679, 326.907)$, for IH. Besides, in the 1σ range [1], $\delta^\circ_{\rm CP} \in (173, 224)$ for NH and $\delta^\circ_{\rm CP} \in (252, 308)$ for IH, while in the 3σ range [1], $\delta^\circ_{\rm CP} \in (120, 369)$ for NH and $\delta^\circ_{\rm CP} \in (193, 352)$ for IH. Hence, this model predicts the Dirac CP violating phase (δ) in which for NH, δ is in 3σ range, and for IH, δ is in 1σ range, of the best-fit values taken from Ref. [1].

In order to fix the parameters, we should deal with the central values given in Table 1. For NH, taking the central values of θ_{23} and θ_{13} as shown in Table 1, $s_{23} = 0.757$, $s_{13} = 0.149$. For IH, taking the central values of θ_{13}, $s_{13} = 0.1496$ and $s_{23} = 0.7517$, which are in the 1σ range of the best-fit value taken from Ref. [1]. We get:

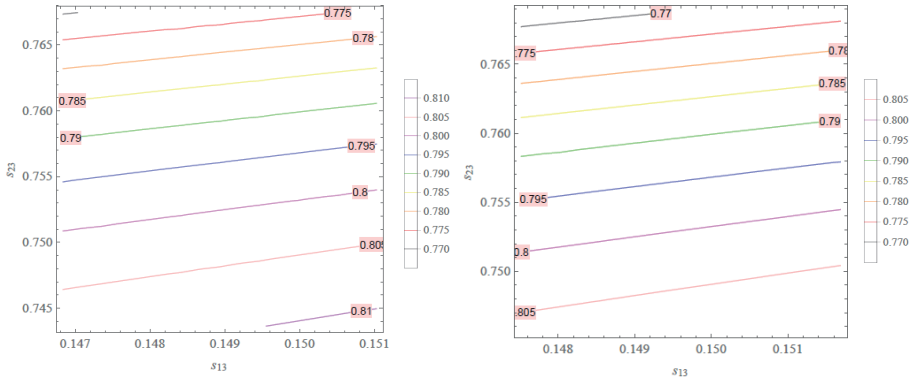

Fig. 1. (color online) Contour plot of $\cos\theta$ as a function of s_{13} and s_{23} in the 1σ range of the best-fit value taken from Ref. [1], i.e. $s_{13} \in (0.1468, 0.1510)$ and $s_{23} \in (0.7436, 0.7675)$ for NH (left), and $s_{13} \in (0.1475, 0.1517)$ and $s_{23} \in (0.7457, 0.7688)$ for IH (right).

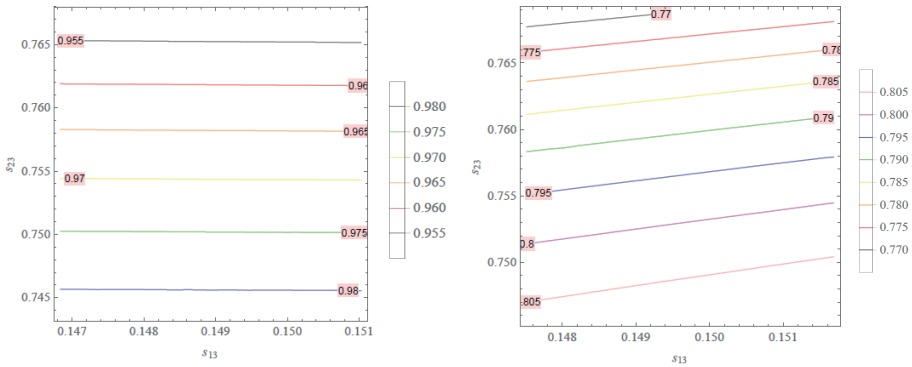

Fig. 2. (color online) Contour plot of $\cos\alpha$ as a function of s_{13} and s_{23} in the 1σ range of the best-fit value taken from Ref. [1], i.e. $s_{13} \in (0.1468, 0.1510)$ and $s_{23} \in (0.7436, 0.7675)$ for NH (left), and $s_{13} \in (0.1475, 0.1517)$ and $s_{23} \in (0.7457, 0.7688)$ for IH (right).

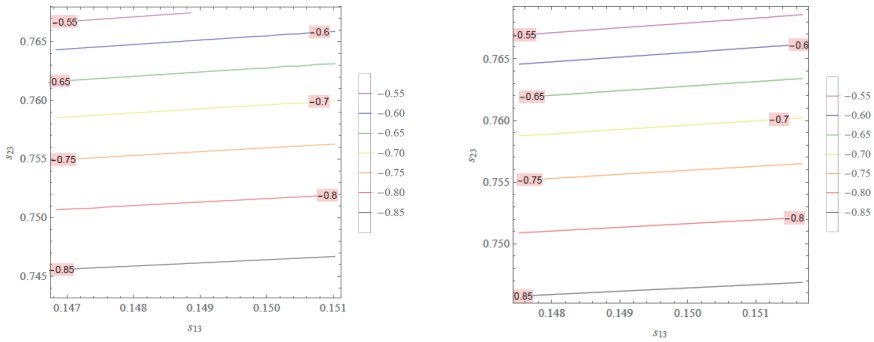

Fig. 3. (color online) Contour plot of $\sin\delta$ as a function of s_{13} and s_{23} in the 1σ range of the best-fit value taken from Ref. [1], i.e. $s_{13} \in (0.1468, 0.1510)$ and $s_{23} \in (0.7436, 0.7675)$ for NH (left), and $s_{13} \in (0.1475, 0.1517)$ and $s_{23} \in (0.7457, 0.7688)$ for IH (right).

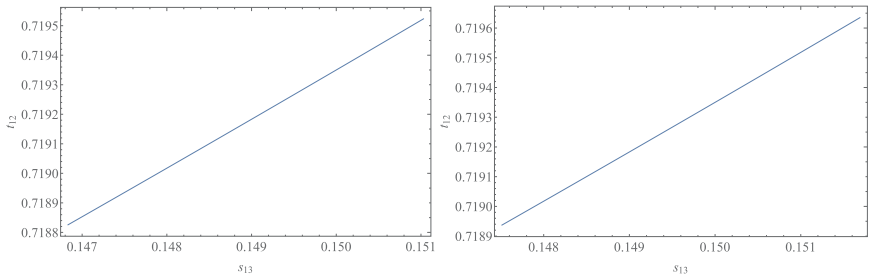

Fig. 4. (color online) t_{12} versus s_{13} with $s_{13} \in (0.1468, 0.1510)$ for NH (left) and $s_{13} \in (0.1475, 0.1517)$ for IH (right) for the 1σ range of the best-fit value taken from Ref. [1].

$$\theta = \begin{cases} 37.47^\circ \text{ for NH}, \\ 53.28^\circ \text{ for IH}, \end{cases} \quad \alpha = \begin{cases} 14.84^\circ \text{ for NH}, \\ 166.70^\circ \text{ for IH} \end{cases} \quad \delta = \begin{cases} 312.91^\circ \text{ for NH}, \\ 307.03^\circ \text{ for IH}, \end{cases} \quad \theta_{12} = \begin{cases} 35.72^\circ \text{ for NH}, \\ 35.73^\circ \text{ for IH}. \end{cases} \tag{36}$$

Substituting Eq. (36) into Eq. (23) yields an explicit form of the leptonic mixing matrix:

$$U_{\rm lep} = \begin{cases} \begin{pmatrix} 0.7977-0.08993\mathrm{i} & 0.5774 & 0.1188-0.08993\mathrm{i} \\ 0.3664+0.339\mathrm{i} & -0.2887-0.50\mathrm{i} & -0.5686+0.3069\mathrm{i} \\ 0.2106-0.2490\mathrm{i} & -0.2887+0.50\mathrm{i} & -0.5686-0.4868\mathrm{i} \end{pmatrix} \text{ for NH}, \\ \begin{pmatrix} -0.7956+0.1063\mathrm{i} & 0.5774 & -0.1053-0.1063\mathrm{i} \\ -0.2779-0.1926\mathrm{i} & -0.2887-0.50\mathrm{i} & 0.6624-0.3369\mathrm{i} \\ -0.2779+0.4052\mathrm{i} & -0.2887+0.50\mathrm{i} & 0.4783+0.4432\mathrm{i} \end{pmatrix} \text{ for IH}. \end{cases} \tag{37}$$

It has been checked that both forms of the leptonic mixing matrix $U_{\rm lep}$ given in Eq. (37) are unitary and consistent with the constraint given in Ref. [1].

As a consequence, the Jarlskog invariant is given by

$$J_{\rm CP} = \begin{cases} -2.501\times10^{-2} \text{ for NH}, \\ -2.744\times10^{-2} \text{ for IH}. \end{cases} \tag{38}$$

From the above analysis, we can conclude that the model under consideration can reproduce the recent experimental values of neutrino mixing angles and Dirac CP violating phase [1] in which the atmospheric angle (θ_{23}) and the reactor angle (θ_{13}) get the best-fit values while the solar angle (θ_{12}) and Dirac CP violating phase (δ) are in 3σ range of the best-fit value for the NH. For the IH, θ_{13} has the best-fit value and θ_{23} together with δ are in the 1σ range, while θ_{12} is in 3σ range of the best-fit value taken from Ref. [1]. Although the model results for t_{12} and δ are in the 3σ range of the best-fit value from Ref. [1], they are within 2σ of the best-fit value taken from Ref. [70] and 1σ of the best-fit value taken from the SNO and KamLAND collaborations [71, 72]. Now we turn to the neutrino mass hierarchy.

A. Normal spectrum

Taking into account the best-fit values of the neutrino mass-squared differences for NH given in Table 1, $\Delta m^2_{21} = 7.42\times10^{-5}\text{eV}^2$, $\Delta m^2_{31} = 2.517\times10^{-3}\text{eV}^2$, we obtain a solution:

$$\kappa_1 = \frac{\sum m_i}{2} - \frac{c_0}{2}, \quad \kappa_2 = \frac{1}{2}\left(\sqrt{\delta_{1N}} - \sqrt{\delta_{2N}}\right), \tag{39}$$

$$c_0 = \frac{\sum m_i}{3} - 132.40\delta_{1N}\sqrt{\delta_{1N}} + 2.102 \times 10^{-5}\left(\sqrt{\delta_{1N}} + \sqrt{\delta_{2N}}\right)\sqrt[3]{\delta_N} + \sqrt{\delta_{2N}}\left[132.4\delta_{2N} - 0.3137 - 264.90\left(\sum m_i\right)^2\right] + \frac{\left(\sqrt{\delta_{1N}} + \sqrt{\delta_{2N}}\right)\delta_{3N}}{\sqrt[3]{\delta_N}}, \quad (40)$$

where δ_N and $\delta_{iN}\,(i=1-4)$ are given in Appendix A. Equations (17), (39), (40) and (A1)-(A5) show that the three neutrino masses $m_{1,2,3}$ depend only on the sum of neutrino masses $\sum_{i=1}^{3} m_i$.

At present there are various bounds on $\sum m_i$. For instance, for the NH, the upper limit on the sum of neutrino masses is $\sum m_i < 0.13$ eV in the 2σ range [70]. The dependence of $m_{1,2,3}$ on $\sum m_i$ is plotted in Fig. 5 with $\sum m_i \in (0.06, 0.1)$ eV within 2σ range of the best-fit value taken from Ref. [70] and being well consistent with the strongest bound from cosmology [73] $\sum m_\nu < 0.078$ eV; the upper bounds are taken from Ref. [74] $\sum m_\nu < 0.12 - 0.69$ eV, and the constraint in Ref. [75] is $\sum m_\nu \in (0.06, 0.118)$ eV. In the case $\sum m_i = 6.5\times10^{-2}$ eV we get:

$$\begin{aligned} m_1 &= 4.76\times10^{-3}\,\text{eV},\\ m_2 &= 9.84\times10^{-3}\,\text{eV},\\ m_3 &= 5.04\times10^{-2}\,\text{eV}. \end{aligned} \quad (41)$$

B. Inverted spectrum

As before, using the best-fit values of the neutrino mass-squared differences for the IH shown in Table 1, $\Delta m^2_{21} = 7.42\times10^{-5}$ eV^2, $\Delta m^2_{32} = -2.498\times10^{-3}$ eV^2, we get a solution:

$$\begin{aligned} \kappa_1 &= \frac{\sum m_i}{2} - \frac{c_0}{2},\\ \kappa_2 &= \frac{1}{2}\left(\sqrt{\delta_{1I}} - \sqrt{\delta_{2I}}\right), \end{aligned} \quad (42)$$

$$c_0 = \frac{\sum m_i}{3} - 137.50\delta_{1I}\sqrt{\delta_{1I}} + 2.183 \times 10^{-5}\left(\sqrt{\delta_{1I}} + \sqrt{\delta_{2I}}\right)\sqrt[3]{\delta_I} + \sqrt{\delta_{2I}}\left[137.50\delta_{2I} + 0.3537 - 275.10\left(\sum m_i\right)^2\right] + \frac{\left(\sqrt{\delta_{1I}} + \sqrt{\delta_{2I}}\right)\delta_{3I}}{\sqrt[3]{\delta_I}}, \quad (43)$$

where δ_I and $\delta_{iI}\,(i=1-4)$ are given in Appendix A. Similar to the previous section, the three neutrino masses $m_{1,2,3}$ just depend on the sum of neutrino masses $\sum_{i=1}^{3} m_i$. For the IH, the tightest 2σ upper limit on the sum of neutrino masses is $\sum m_i < 0.15$ eV [70]. Furthermore, the upper bound taken from Ref. [74] is $\sum m_\nu < 0.12 - 0.69$ eV, while the constraint given in Ref. [75] is $\sum m_\nu \in (0.1, 0.151)$ eV. The dependence of the three active neutrino masses $m_{1,2,3}$ on $\sum m_i$ is plotted in Fig. 6 with $\sum m_i \in (0.1, 0.2)$ eV, which is well consistent with the recent constraints given in Refs. [70, 74, 75]. In the case $\sum m_i = 0.1075$ eV we get:

$$\begin{aligned} m_1 &= 4.976\times10^{-2}\,\text{eV},\\ m_2 &= 5.05\times10^{-2}\,\text{eV},\\ m_3 &= 7.237\times10^{-3}\,\text{eV}. \end{aligned} \quad (44)$$

C. Effective neutrino mass parameters

Now, we deal with an effective neutrino mass. Equations (17), (39), (40) and (A1)-(A5) (for NH) and (17), (42), (43) and (A6)-(A10) (for IH) show that, with the best-fit values of the neutrino mass-squared differences, the effective neutrino mass parameters $\langle m_{ee}\rangle$ and m_β depend on the sum of neutrino masses $\sum_{i=1}^{3} m_i$ and two mixing angles θ_{23}, θ_{13}. In the NH, $m_1 < m_2 < m_3$, hence $m_1 \equiv m_{\text{light}}$ is the lightest neutrino mass, while in the IH, $m_3 < m_1 < m_2$, therefore $m_3 \equiv m_{\text{light}}$ is the lightest neutrino mass. If we fix θ_{23} and θ_{13} at their best-fit values taken in Table 1, the effective neutrino masses $\langle m_{ee}\rangle$, m_β and m_{light} as functions of $\sum m_i$ are as plotted in Fig. 7.

In order to see the dependence of $\langle m_{ee}\rangle$ and m_β on θ_{23} and θ_{13} we can fix the value for $\sum m_i$ in its constraint

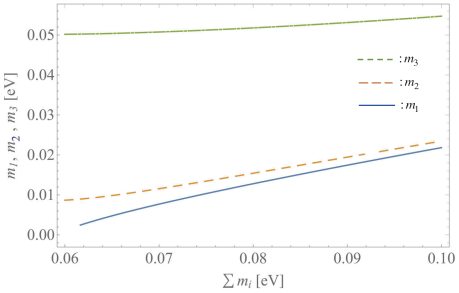

Fig. 5. (color online) $m_{1,2,3}$ versus $\sum m_i$ with $\sum m_i \in (0.06, 0.1)$ eV in the NH.

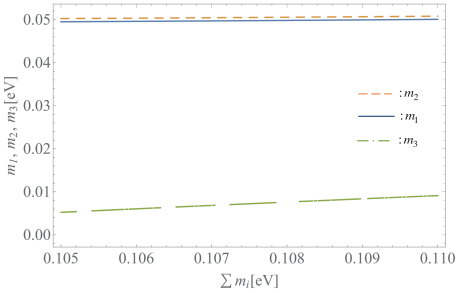

Fig. 6. (color online) $m_{1,2,3}$ versus $\sum m_i$ with $\sum m_i \in (0.105, 0.11)$ eV in the IH.

range [70, 74]. For instance, $\sum m_i = 0.065$ eV for NH and $\sum m_i = 0.1075$ eV for IH. Consequently, we can contour plot $\langle m_{ee}\rangle$ and m_β as functions of $(\theta_{23}, \theta_{13})$, as shown in Figs. 8 and 9, respectively.

These figures show that at 1σ range of the best-fit value taken from Ref. [1] of s_{23} and s_{13}, the model predicts the range of the effective neutrino mass parameters as follows:

$$\langle m_{ee}\rangle \in \begin{cases} (6.40,\ 7.10)\ \text{meV} & \text{for NH}, \\ (48.04,\ 48.64)\ \text{meV} & \text{for IH}, \end{cases} \tag{45}$$

and

$$m_\beta \in \begin{cases} (10.10,\ 10.22)\ \text{meV} & \text{for NH}, \\ (49.45,\ 49.48)\ \text{meV} & \text{for IH}. \end{cases} \tag{46}$$

In the case where s_{23} and s_{13} take their best-fit values [1], $s_{23} = 0.757$, $s_{13} = 0.149$ for NH and for $s_{23} = 0.7583$, $s_{13} = 0.1496$IH, one gets:

$$\langle m_{ee}\rangle = \begin{cases} 6.81\ \text{meV} & \text{for NH}, \\ 48.48\ \text{meV} & \text{for IH}, \end{cases} \tag{47}$$

and

$$m_\beta = \begin{cases} 10.20\ \text{meV} & \text{for NH}, \\ 49.46\ \text{meV} & \text{for IH}. \end{cases} \tag{48}$$

The derived effective neutrino mass parameters in Eqs. (47) and (48) satisfy all the upper bounds arising from recent $0\nu\beta\beta$ decay experiments taken from KamLAND-Zen [76] $\langle m_{ee}\rangle < 61 - 165$ meV, GERDA [77] $\langle m_{ee}\rangle < 104 - 228$ meV and CUORE [78] $\langle m_{ee}\rangle < 75 - 350$ meV.

V. CONCLUSIONS

We have suggested a multiscalar and nonrenormaliz-

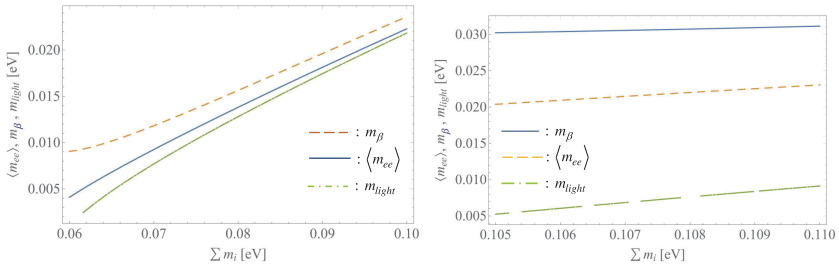

Fig. 7. (color online) $\langle m_{ee}\rangle$, m_β and m_{light} versus $\sum m_i$ with $\sum m_i \in (0.06,\ 0.1)$ eV in the NH (left) and $\sum m_i \in (0.105,\ 0.11)$ eV in the IH (right).

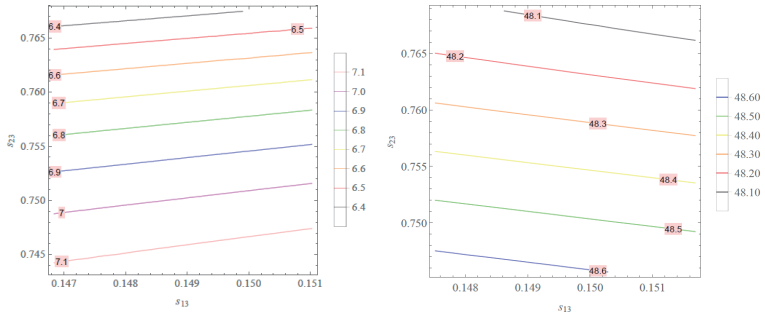

Fig. 8. (color online) Contour plot of $\langle m_{ee}\rangle$(meV) as a function of s_{13} and s_{23} in the 1σ range of the best-fit values: $s_{13} \in (0.1468,\ 0.1510)$ and $s_{23} \in (0.7436,\ 0.7675)$ for NH (left), and $s_{13} \in (0.1475,\ 0.1517)$ and $s_{23} \in (0.7457,\ 0.7688)$ for IH (right).

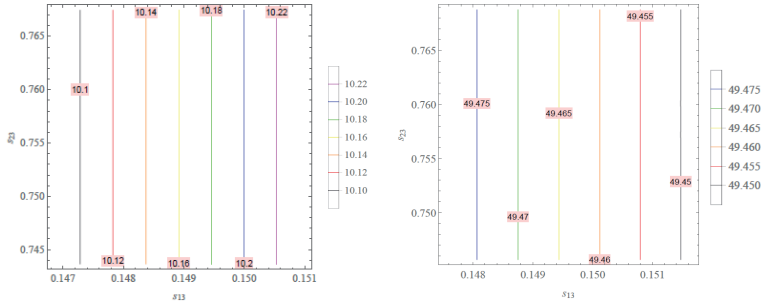

Fig. 9. (color online) Contour plot of m_β(meV) as a function of s_{13} and s_{23} in the 1σ range of the best-fit values: $s_{13} \in (0.1468,\ 0.1510)$ and $s_{23} \in (0.7436,\ 0.7675)$ for NH (left), and $s_{13} \in (0.1475,\ 0.1517)$ and $s_{23} \in (0.7457,\ 0.7688)$ for IH (right).

able $U(1)_{B-L}$ extension of the SM with S_4 symmetry which successfully explains the recent observed neutrino oscillation data. The tiny neutrino mass and the neutrino mass hierarchies are generated via the type-I seesaw mechanism. The model reproduces the recent experimental data of neutrino mixing angles and Dirac CP violating phase in which the atmospheric angle (θ_{23}) and the reactor angle (θ_{13}) get the best-fit values while the solar angle (θ_{12}) and Dirac CP violating phase (δ) are in 3σ range of the best-fit value for the NH. For the IH, θ_{13} gets the best-fit value and θ_{23} together with δ are in the 1σ range, while θ_{12} belongs to 3σ range of the best-fit value. The effective neutrino masses are predicted to be $\langle m_{ee}\rangle = 6.81$ meV for the NH and $\langle m_{ee}\rangle = 48.48$ meV for the IH, while $m_\beta = 10.20$ meV for the NH and $m_\beta = 49.46$ meV for the IH, which are strongly consistent with the most recent experimental data.

APPENDIX A: EXPLICIT EXPRESSION OF $\delta_{N(I)}$ AND $\delta_{iN(I)}\,(i=1-4)$

The parameters $\delta_{N(I)}$ and $\delta_{iN(I)}\,(i=1-4)$ in Eqs. (39), (40), (42), (43) have explicit expressions as follows:

$$\delta_{1N} = 7.895\times10^{-4} + 5.291\times10^{-8}\sqrt[3]{\delta_N} + \frac{2}{3}\left(\sum m_i\right)^2 - \frac{26.99 - 4979\,(\sum m_i)^2 - 2.10\times10^6\,(\sum m_i)^4}{\sqrt[3]{\delta_N}}, \tag{A1}$$

$$\delta_{2N} = 1.5795\times10^{-3} + 5.291\times10^{-8}\sqrt[3]{\delta_N} + \frac{4}{3}\left(\sum m_i\right)^2 + \frac{26.99 - 4979\,(\sum m_i)^2 - 2.10\times10^6\,(\sum m_i)^4}{\sqrt[3]{\delta_N}} + \frac{5.034\times10^{-3}\sum m_i}{\sqrt{\delta_{1N}}}, \tag{A2}$$

$$\delta_{3N} = -1.0722\times10^4 + 1.976\times10^6\left(\sum m_i\right)^2 + 8.343\times10^8\left(\sum m_i\right)^4, \tag{A3}$$

$$\delta_N = -1.308\times10^{13} + 9.639\times10^{15}\left(\sum m_i\right)^2 - 8.882\times10^{17}\left(\sum m_i\right)^4 - 2.50\times10^{20}\left(\sum m_i\right)^6 - 6.539\times10^{12}\sqrt{\delta_{4N}}, \tag{A4}$$

$$\delta_{4N} = 7.101 - 7.61\times10^3\left(\sum m_i\right)^2 + 2.308\times10^6\left(\sum m_i\right)^4 - 6.65\times10^{10}\left(\sum m_i\right)^8. \tag{A5}$$

$$\delta_{1I} = -8.574\times10^{-4} + 5.291\times10^{-8}\sqrt[3]{\delta_I} + \frac{2}{3}\left(\sum m_i\right)^2 - \frac{24.28 + 5401\,(\sum m_i)^2 - 2.10\times10^6\,(\sum m_i)^4}{\sqrt[3]{\delta_I}}, \tag{A6}$$

$$\delta_{2I} = -1.715\times10^{-3} - 5.291\times10^{-8}\sqrt[3]{\delta_I} + \frac{4}{3}\left(\sum m_i\right)^2 + \frac{24.28 + 5401\,(\sum m_i)^2 - 2.10\times10^6\,(\sum m_i)^4}{\sqrt[3]{\delta_I}} - \frac{4.848\times10^{-3}\sum m_i}{\sqrt{\delta_{1I}}}, \tag{A7}$$

$$\delta_{3I} = -1.002\times10^4 - 2.228\times10^6\left(\sum m_i\right)^2 + 8.664\times10^8\left(\sum m_i\right)^4, \tag{A8}$$

$$\delta_I = 1.328\times10^{13} + 8.673\times10^{15}\left(\sum m_i\right)^2 + 9.646\times10^{17}\left(\sum m_i\right)^4 - 2.50\times10^{20}\left(\sum m_i\right)^6 - 6.297\times10^{12}\sqrt{\delta_{4I}}, \tag{A9}$$

$$\delta_{4I} = 6.886 + 7.436\times10^3\left(\sum m_i\right)^2 + 2.273\times10^6\left(\sum m_i\right)^4 - 6.25\times10^{10}\left(\sum m_i\right)^8. \tag{A10}$$

References

[1] I. Esteban, M. Gonzalez-Garcia, M. Maltoni *et al.*, J. High Energy Phys. **09**, 178 (2020), arXiv:2007.14792
[2] A. Davidson, Phys. Rev. D **20**, 776 (1979)
[3] R. N. Mohapatra and R. E. Marshak, Phys. Rev. Lett. **44**, 1316 (1980)
[4] R. E. Marshak and R. N. Mohapatra, Phys. Lett. **91B**, 222 (1980)
[5] C. Wetterich, Nucl. Phys. B **187**, 343 (1981)
[6] A. Masiero, J. F. Nieves, and T. Yanagida, Phys. Lett. **116 B**, 11 (1982)
[7] S. Khalil, J. Phys. **G35**, 055001 (2008), arXiv:hep-ph/0611205
[8] S. Khalil and H. Okada, Phys. Rev. D **79**(08), 3510 (2009), arXiv:0810.4573
[9] A. Das, N. Okada, S. Okada *et al.*, Phys. Lett. B **797**, 134849 (2019), arXiv:1812.11931
[10] J. C. Gómez-Izquierdo and M. Mondragón, Eur. Phys. J. C **79**, 285 (25019)

[11] V. V. Vien, J. Phys. G: Nucl. Part. Phys. **47**, 055007 (2020)
[12] V. V. Vien, Nucl. Phys. B **956**, 115015 (2020)
[13] T. Araki et. al., Nucl. Phys. B **805**, 124 (2008), arXiv:0805.0207
[14] T. Kobayashi *et al*., J. High Energy Phys. **02**, 097 (2020), arXiv:1907.09141
[15] H. Ishimori *et al*., Lect. Notes Phys. **858**, 1 (2012)
[16] G. Altarelli, F. Feruglio, and L. Merlo, J. High Energy Phys. **0905**, 020 (2009), arXiv:0903.1940
[17] F. Bazzocchi, L. Merlo, and S. Morisi, Phys. Rev. D **80**, 053003 (2009), arXiv:0902.2849
[18] F. Bazzocchi, L. Merlo, and S. Morisi, Nucl. Phys. B **816**, 204 (2009), arXiv:0901.2086
[19] R. de Adelhart Toorop, F. Bazzocchi, and L. Merlo, J. High Energy Phys. **1008**, 001 (2010), arXiv:1003.4502
[20] K. M. Patel, Phys. Lett. B **695**, 225 (2011), arXiv:1008.5061
[21] H. Ishimori, Y. Shimizu, M. Tanimoto *et al*., Phys. Rev. D **83**, 033004 (2011), arXiv:1010.3805
[22] P. V. Dong, H. N. Long, D. V. Soa *et al*., Eur. Phys. J. C **71**, 1544 (2011)
[23] S. Morisi, K. M. Patel, and E. Peinado, Phys. Rev. D **84**, 053002 (2011), arXiv:1107.0696
[24] C. Hagedorn and M. Serone, J. High Energy Phys. **1110**, 083 (2011), arXiv:1106.4021
[25] G. Altarelli, F. Feruglio, L. Merlo *et al*., J. High Energy Phys. **1208**, 021 (2012), arXiv:1205.4670
[26] R. N. Mohapatra and C. C. Nishi, Phys. Rev. D **86**, 073007 (2012), arXiv:1208.2875
[27] P. S. Bhupal Dev, B. Dutta, R. N. Mohapatra *et al*., Phys. Rev. D **86**, 035002 (2012)
[28] I. de Medeiros Varzielas, and L. Lavoura, J. Phys. G **40**, 085002 (2013), arXiv:1212.3247
[29] G. J. Ding, S. F. King, C. Luhn *et al*., J. High Energy Phys. **1305**, 084 (2013), arXiv:1303.6180
[30] G. J. Ding and Y. L. Zhou, Nucl. Phys. B **876**, 418 (2013), arXiv:1304.2645
[31] A. E. Cárcamo Hernández, Nicolás A. Pérez-Julve, and Yocelyne Hidalgo Velásquez, Phys. Rev. D **100**, 095025 (2019), arXiv:1907.13083
[32] V. V. Vien and H. N. Long, Adv. High Energy Phys. **2014**, 192536 (2014)
[33] V. V. Vien, H. N. Long, and D. P. Khoi, Int. J. Mod. Phys. A **30**, 1550102 (2015), arXiv:1506.06063
[34] V. V. Vien, Int. J. Mod. Phys. A **31**, 1650039 (2016), arXiv:1603.03933
[35] F. J. de Anda, S. F. King, and E. Perdomo, J. High Energy Phys. **12**, 075 (2017), arXiv:1710.03229
[36] F. J. de Anda and S. F. King, J. High Energy Phys. **1807**, 057 (2018), arXiv:1803.04978[hep-ph]
[37] I. De Medeiros Varzielas, M. Levy *et al*., Phys. Rev. D **100**, 035027 (2019), arXiv:1903.10506
[38] P. T. Chen, G. J. Ding, S. F. King *et al*., J. Phys. G: Nucl. Part. Phys. **47**, 065001 (2020), arXiv:1906.11414
[39] V. V. Vien, H. N. Long and A. E. Cárcamo Hernández, Prog. Theor. Exp. Phys. **2019**, 113B04 (2019), arXiv:1909.09532
[40] S. Petcov and A. Titov, Phys. Rev. D **97**, 115045 (2018), arXiv:1804.00182
[41] A. E. Cárcamo Hernández and S. F. King, Nucl. Phys. B **953**, 114950 (2020), arXiv:1903.02565
[42] L. Lavoura, Eur. Phys. J. **C29**, 191 (2003)
[43] L. T. Hue, L. D. Ninh, T. T. Thuc *et al*., Eur. Phys. J. C **78**, 128 (2018)
[44] M. D. Campos, A. E. Cárcamo Hernández, H. Päs *et al*., Phys. Rev. D **91**, 116011 (2015)
[45] M. Lindner, M. Platscher, and F. S. Queiroz, Phys. Rept. **731**, 1 (2018)
[46] P. A. Zyla *et al*. (Particle Data Group), Prog. Theor. Exp. Phys. **2020**, 083C01 (2020)
[47] B. Pontecorvo, Zh. Eksp. Teor. Fiz. **33**, 549 (1957)
[48] B. Pontecorvo, Zh. Eksp. Teor., Fiz. **34**, 247 (1958)
[49] Z. Maki, M. Nakagawa, and S. Sakata, Prog. Theor. Phys. **28**, 870 (1962)
[50] P. I. Krastev and S. T. Petcov, Phys. Lett. B **205**, 84 (1988)
[51] W. Rodejohann, Phys. Rev. D **69**, 033005 (2004)
[52] C. Jarlskog, Phys. Rev. Lett. **55**, 1039 (1985)
[53] D. -d. Wu, Phys. Rev. D **33**, 860 (1986)
[54] O. W. Greenberg, Phys. Rev. D **32**, 1841 (1985)
[55] M. Mitra, G. Senjanovic, and F. Vissani, Nucl. Phys. B **856**, 26 (2012), arXiv:1108.0004
[56] W. Rodejohann, J. Phys. G **39**, 124008 (2012), arXiv:1206.2560
[57] J. D. Vergados, H. Ejiri, and F. Simkovic, Rep. Prog. Phys. **75**, 106301 (2012), arXiv:1205.0649
[58] K. Fukuura, T. Miura, E. Takasugi *et al*., Phys. Rev. D **61**, 073002 (2000), arXiv:hepph/9909415
[59] T. Miura, E. Takasugi, and M. Yoshimura, Phys. Rev. D **63**, 013001 (2001), arXiv:hep-ph/0003139
[60] E. Ma, Phys. Rev. D **66**, 117301 (2002), arXiv:hep-ph/0207352
[61] X. -G. He, Chin. J. Phys. **53**, 100101 (2015), arXiv:1504.01560
[62] E. Ma, Phys. Lett. B **752**, 198 (2016), arXiv:1510.02501
[63] E. Ma, Phys. Lett. B **755**, 348 (2016), arXiv:1601.00138
[64] E. Ma and G. Rajasekaran, Europhys. Lett. **119**(3), 31001 (2017), arXiv:1708.02208
[65] E. Ma, Phys. Lett. B **777**, 332 (2018), arXiv:1707.03352
[66] W. Grimus and L. Lavoura, Phys. Lett. B **774**, 325 (2017), arXiv:1708.09809
[67] E. Ma, Eur. Phys. J. C **79**(11), 903 (2019), arXiv:1905.01535
[68] E. Ma, Nucl. Phys. B **946**, 114725 (2019), arXiv:1907.04665
[69] A. E. Cárcamo Hernández and Ivo de Medeiros Varzielas, Phys. Lett. B **806**, 135491 (2020), arXiv:2003.01134
[70] P. F. de Salas *et al*., J. High Energ. Phys. **2021**, 71 (2021), arXiv: 2006.11237
[71] S. Abe *et al*. (KamLAND Collaboration), Phys. Rev. Lett. **100**, 221803 (2008), arXiv:0801.4589
[72] B. Aharmim *et al*. (SNO Collaboration), Phys. Rev. C **72**, 055502 (2005)
[73] S. Roy Choudhury and S. Choubey, JCAP **1809**(09), 017 (2018), arXiv:1806.10832
[74] F. Capozzi, S. S. Chatterjee, and A. Palazzo, Phys. Rev. Lett. **124**(11), 111801 (2020)
[75] S. Vagnozzi *et al*., Phys. Rev. D **96**, 123503 (2017), arXiv:1701.08172
[76] A. Gando *et al*. (KamLAND-Zen Collaboration), Phys. Rev. Lett. **117**(8), 082503 (2016)
[77] M. Agostini *et al*. (GERDA Collaboration), Science **365**, 1445 (2019), arXiv:1909.02726
[78] D. Adams *et al*. (CUORE collaboration), Phys. Rev. Lett. **124**, 122501 (2020), arXiv:1912.10966